
MIXFACE: IMPROVING FACE VERIFICATION FOCUSING ON FINE-GRAINED CONDITIONS

Junuk Jung, Sungbin Son, Joochan Park, Yongjun Park, Seonhoon Lee, Heung-Seon Oh*

School of Computer Science and Engineering

Korea University of Technology and Education (KOREATECH)

{rnans33, sbson0621, green669, qkr2938, karma1002, ohhs}@koreatech.ac.kr

ABSTRACT

The performance of face recognition (FR) has become saturated for public benchmark datasets such as LFW, CFP-FP, and AgeDB, owing to the rapid advances in CNNs. However, the effects of faces with various fine-grained conditions on FR models have not been investigated because of the absence of such datasets. This paper analyzes their effects in terms of different conditions and loss functions using K-FACE, a recently introduced FR dataset with fine-grained conditions. We propose a novel loss function, MixFace², that combines classification and metric losses. The superiority of MixFace in terms of effectiveness and robustness is demonstrated experimentally on various benchmark datasets.

Keywords Face Recognition · Face Verification

1 Introduction

Face recognition (FR) is one of the most promising computer vision tasks and is widely utilized in surveillance and security. Recently, FR has achieved remarkable results on benchmark datasets owing to advances in CNNs [1, 2, 3, 4]. Based on CNNs, there are three major FR research directions: 1) denoising FR data [5], 2) improving face detection and face alignment [6], and 3) devising novel loss functions [7, 8, 9, 10, 11, 12]. Among them, the third direction has gained the attention of many researchers.

Loss functions in FR can be categorized into two approaches: classification and metric losses. The former optimizes the similarity between the deep feature and weight vectors using class labels. Softmax loss [7, 10, 12] is a typical example of a classification loss. The latter optimizes the similarity between deep feature vectors using pairwise labels. Contrastive loss [8, 9] and triplet loss [11] belong to the metric loss category. Although both approaches have contributed to improving FR considerably, each has limitations. Softmax loss performs well in the closed-set protocol where test classes are represented in the training set but poorly in the open-set protocol where test classes are disjoint from the training set because of a lack of discriminative power [13]. Contrastive loss and triplet loss have slow convergence and reach local optima [14] because a limited number of face combinations are used in each training iteration, even over a tremendous number of possible face combinations from a FR dataset. In addition, they cannot distinguish difficult samples because FR models are trained with easy samples in repetition [15].

To address these problems, for classification loss, softmax loss functions using angular margins [16, 17, 18, 19] were presented to obtain a discriminative power satisfying intra-class compactness and inter-class dispersion. In particular, ArcFace [16] improved FR by directly giving margins to the arc degree between the deep feature and target weight vectors. For metric loss, various sampling

*corresponding author

²Codes are available at <https://github.com/Jung-Jun-Uk/mixface.git>

strategies have been studied to increase the number of face combinations in a training iteration [14] and alleviate the domination of easy samples [15, 11, 20, 21]. Both approaches use normalization to the deep feature vectors. Moreover, for classification loss, weight vectors are normalized to obtain a precise cosine similarity space [16, 17, 19, 15, 22, 23], and a scale factor is used to distinguish subtle differences between these similarities. Research on classification loss has gained more attention because it is difficult to alleviate inefficiency in metric loss. Accuracy greater than 99% accuracy has been achieved on several benchmark datasets (LFW [24], CFP-FP [25], and AgeDB [26]).

However, it has been infeasible to investigate the effects of faces with fine-grained conditions such as varying lighting, poses, accessories, and facial expressions on FR in previous research due to the lack of such datasets. An in-depth analysis of fine-grained conditions is essential to improve robust FR models. Recently, the K-FACE [27] dataset, which contains fine-grained conditions, was introduced to improve FR research. We analyzed the performance of classification and metric loss functions on this dataset. The analysis showed that the two approaches lack the representation power to adequately accommodate the changes in conditions, but we hypothesized that the two approaches could be combined.

Therefore, we propose a novel loss function, MixFace, that combines classification and metric losses. MixFace uses scale factors s_1 and s_2 for the two approaches. We assumed that manual tuning would not guarantee proper harmony in MixFace because they have different ranges. Therefore, we present a unified scale factor ϵ derived from ideal similarities of the classification and metric losses such that a hyper-parameter easily determines s_1 and s_2 . Our experimental results demonstrate the superiority of MixFace in terms of two aspects. First, MixFace is effective because it outperforms the existing loss functions with fine-grained conditions. Second, MixFace maintains generalization capability because it achieves competitive performance on benchmark datasets (LFW, CFP-FP, and AgeDB30). The contributions of this paper can be summarized as follows:

- This paper examines the effects of fine-grained conditions in FR using K-FACE in terms of both training and testing, as well as classification and metric losses.
- This paper proposes a novel loss function, MixFace, that combines classification and metric losses. It inherits the benefits and complements the weaknesses of the two approaches. Exhaustive experiments show the superiority of MixFace in terms of effectiveness and robustness.

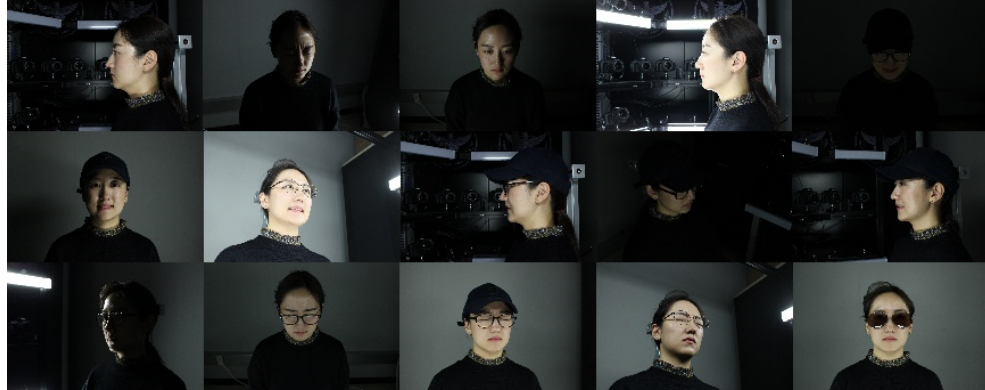


Figure 1: K-FACE sample images with various conditions.

2 K-FACE Dataset

2.1 Summary of the K-FACE

K-FACE [27] is a FR dataset consisting of 17,550,000 ($1000 \times 6^+ \times 29 \times 3 \times 20$) images of 1,000 subjects with more than six accessories, 35 lights, three facial expressions, and 27 poses. Owing to privacy and disclosure issues, only a subset of K-FACE consisting of 4,176,600 ($400 \times 6 \times 29 \times 3 \times 20$) images of 400 subjects with six accessories, 29 lights, three facial expressions, and 20 poses are

available. A condition indicates an instance of four attributes and has a fine granularity due to many combinations. Table 1 summarizes the configuration of the dataset we used, and sample images with various conditions are shown in Figure 1. In the remainder of this paper, “K-FACE” denotes the subset used.

Table 1: Configuration of K-FACE.

Pose			Illumination				
Label	Direction		Label	Direction			
	Vertical	Horizontal		Vertical	Horizontal		
C1	0	+90	All	L1	1000		
C2		+75		L2	400		
C3		+60		L3	200		
C4		+45		L4	150		
C5		+30		L5	100		
C6		+15		L6	40		
C7		0		L7	0		
C8		-15		L8	400		
C9		-30		L9	200		
C10		-45		L10	100		
C11		-60		L11	40		
C12		-75		L12	400		
C13		-90		L13	200		
C14	+30	+45	All	L14	100		
C15		+30		L15	40		
C16		+15		L16	400		
C17		0		L17	200		
C18		-15		L18	100		
C19		-30		L19	40		
C20		-45		L20	400		
Label		Accessories			+90		
A1		Neutral					
A2		Glasses					
A3		Horn-rimmed glasses					
A4		Sunglasses					
A5		Cap					
A6		Cap + Horn-rimmed glasses			+45		
Label		Expression					
E1		Neutral					
E2		Smile					
E3		Disgust					

Table 2: Training and test datasets with different variances of conditions. Accessories, Lux, Expression, and Pose.

Train ID	A	L	E	P	#Images	Variance
T ₁	A1	1000	E1	C4 – 10	2,590	Very Low
T ₂	A1 – 2	400 – 1000	E1	C4 – 10	46,620	Low
T ₃	A1 – 4	200 – 1000	E1 – 2	C4 – 13	654,160	Middle
T ₄	A1 – 6	40 – 1000	E1 – 3	C1 – 20	3,862,800	High
Test ID	A	L	E	P	# Pairs	Variance
Q ₁	A1	1000	E1	C4 – 10	1,000	Very Low
Q ₂	A1 – 2	400 – 1000	E1	C4 – 10	100,000	Low
Q ₃	A1 – 4	200 – 1000	E1 – 2	C4 – 13	100,000	Middle
Q ₄	A1 – 6	40 – 1000	E1 – 3	C1 – 20	100,000	High

2.2 Data Preparation

Of the 400 subjects in the dataset, 370 and 30 subjects were training and test data, respectively. To analyze the effects of the variances of conditions, four datasets of training and test sets with different degrees of condition variation were constructed, as shown in Table 2. $T_1 - T_4$ and $Q_1 - Q_4$ denote training and test datasets, where the variance of conditions increases with increasing subscript index. The variance of the conditions increases as more conditions (values) are included. Each test dataset consists of positive and negative pairs with a 1:1 ratio, where the positive indicates the two face images belong to the same class, and the negative indicates that they do not. They were randomly sampled without replacement using four attributes from 30 subjects. Table 2 summarizes the training and test datasets with different variances of conditions.

3 Observations

This section analyzes the effects of variances of conditions on the performance of two different loss functions through concrete experiments for face verification, where performance was measured by accuracy. ArcFace [16] and SN-pair loss were chosen for baseline classification and metric losses, respectively, where the SN-pair loss is a similarity-based N-pair loss [14]. ResNet-34 [1] was chosen as the baseline backbone. The details of the two loss functions and implementation are explained in Sections 4 and 5, respectively.

3.1 Effects of Variances of Conditions

Figure 2 shows the results obtained with $T_1 - T_4$ and $Q_1 - Q_4$ as heatmaps; for example, $(T_1, Q_2, 66.2)$ in ArcFace means that the accuracy is 66.2 on Q_2 with a FR model trained with T_1 . Analysis was conducted by partitioning the heatmaps into a lower triangle P_L (red border), a diagonal line P_D (no border), and an upper triangle P_U (blue border). Simply, P_L , P_D , and P_U indicate under-, balanced-, and over-training, respectively, by specifying with and without conditions. Under-training indicates that some conditions are excluded in the training datasets but included in the test datasets; vice versa for over-training. Balanced-training indicates that the same conditions appear in both training and test datasets. We observed several key results. First, under-training must be avoided because of its low performance. Second, the difficulty increases as the variance of conditions increases in the test datasets. In addition, the training dataset with a high variance of conditions, T_4 , results in underperformance in all test datasets compared with others such as T_2 and T_3 . This shows that over-trained models lack representation power from all variances of conditions. In summary, for a robust FR with fine-grained conditions, the representation power of the model must be increased to minimize the performance penalty that occurs on datasets from low to high variance of conditions.

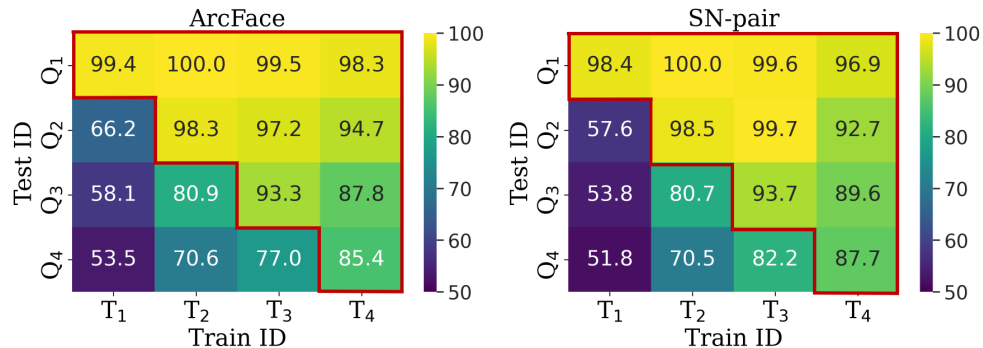


Figure 2: Heatmaps by varying training and test datasets in ArcFace and SN-pair.

3.2 Classification vs. Metric Losses

Figure 3 shows the performance of the classification and metric losses. The test datasets in Table 2 were evaluated using models trained with T_4 . Interestingly, ArcFace shows improvements over SN-Pair in Q_1 and Q_2 , whereas SN-pair achieves better performance in Q_3 and Q_4 . This indicates

that classification loss has strength on low variances, whereas metric loss has strength on high variances. This reveals the importance of metric loss even though research on classification loss became dominant because its superiority was demonstrated on benchmark datasets. This observation motivated the invention of MixFace.

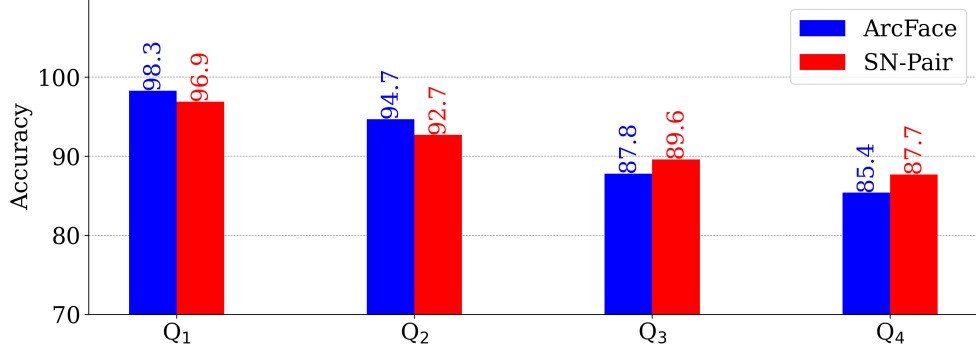


Figure 3: Performance of classification and metric losses on different test datasets.

4 Proposed Loss Function

In this section, after introducing representative loss functions for classification and metric losses, the proposed loss function inheriting their advantages is described.

4.1 Classification Loss: ArcFace

x_i and y_i are a deep feature vector and class-label of i -th face image, respectively, and w_j is a class weight vector of j -th class. Then, softmax loss is defined as:

$$\mathcal{L}_{softmax} = -\frac{1}{N} \sum_{i=1}^N \log \frac{e^{\mathbf{w}_{y_i}^\top \mathbf{x}_i}}{\sum_{j=1}^C e^{\mathbf{w}_j^\top \mathbf{x}_i}} \quad (1)$$

where C is the number of classes and N is the size of the batch.

The research on center loss [13] has indicated that softmax loss is unsuitable for FR because it does not sufficiently satisfy intra-class compactness and inter-class dispersion owing to the lack of discriminative power. Thus, the recently developed classification losses [16, 17, 18, 19] have attempted to increase the discriminative power by incorporating angle margins into $\cos \theta_{i,y_i} = \mathbf{w}_{y_i}^\top \mathbf{x}_i / (\|\mathbf{w}_{y_i}^\top\| \|\mathbf{x}_i\|)$ in various ways. Note that $\cos \theta_{i,y_i}$ is the angle between the deep feature and target weight vectors. ArcFace [16] is a representative classification loss based on softmax using an angular margin:

$$\mathcal{L}_{arc} = -\frac{1}{N} \sum_{i=1}^N \log \frac{e^{s_1 \cdot \cos(\theta_{i,y_i} + m)}}{e^{s_1 \cdot \cos(\theta_{i,y_i} + m)} + \sum_{j=1, j \neq y_i}^C e^{s_1 \cdot \cos \theta_{i,j}}} \quad (2)$$

where s_1 is a scale factor and m is an angular margin.

4.2 Metric Loss: SN-Pair loss

When using metric loss, our concern is $\cos \theta_{i,j} = \mathbf{x}_j^\top \mathbf{x}_i / (\|\mathbf{x}_j^\top\| \|\mathbf{x}_i\|) \in \mathbb{R}^{N \times N}$ where $\cos \theta_{i,j}$ is the angle between the deep feature vectors of the i -th and j -th face images. A pair of two face images is a positive example if they indicate the same person, and a negative example otherwise. They can be extracted from the upper triangle matrix of $\cos \theta_{i,j}$ as:

$$\begin{aligned} \{\cos \theta_k^p\} &= \{\cos \theta_{i,j} \text{ for } i < j \text{ where } y_i = y_j\} \\ \{\cos \theta_l^n\} &= \{\cos \theta_{i,j} \text{ for } i < j \text{ where } y_i \neq y_j\} \end{aligned} \quad (3)$$

where p and n are positive and negative pairs, respectively, and k and l are the indices of the positive and negative pairs, respectively.

N-pair loss [14] was devised to compute the loss of samples in a batch at once to alleviate the problem of insufficient pairs at each training iteration in triplet loss [11]. Recent metric loss functions [28, 15, 23] have employed cosine similarity to reduce the metric gap between training and testing. As a result, the similarity-based N pair loss (SN-pair loss) is defined as:

$$\mathcal{L}_{sn-pair} = \frac{1}{K} \sum_{k=1}^K \log \left(1 + \sum_{l=1}^L e^{s_2 \cdot \cos \theta_l^n - s_2 \cdot \cos \theta_k^p} \right) = -\frac{1}{K} \sum_{k=1}^K \log \frac{e^{s_2 \cdot \cos \theta_k^p}}{e^{s_2 \cdot \cos \theta_k^p} + \sum_{l=1}^L e^{s_2 \cdot \cos \theta_l^n}} \quad (4)$$

where K and L are the numbers of positive and negative examples, respectively, and s_2 is a scale factor.

4.3 MixFace

We have observed that the classification loss has strength on the low variances of conditions, whereas the metric loss has it on the high variances (Section 3). We propose that combining the two losses inherits the benefits and complements each other. As a result, we propose MixFace:

$$\mathcal{L}_{mix} = \mathcal{L}_{arc} + \mathcal{L}_{sn-pair} \quad (5)$$

There are two scale factors, s_1 and s_2 , applicable to ArcFace and SN-Pair loss, respectively. It is essential to adjust the scale factors to improve the performance. Optimizing them using grid and random searches[29] is problematic because it requires huge computational costs owing to their different behaviors. To solve this problem, we devised a unified scale factor used in both ArcFace and SN-Pair loss without loss of generality. The ideal similarities of the positives and negatives are expected to be $\cos(\theta_{i,y_i} + m) \rightarrow 1$ and $\cos \theta_{i,j \neq y_i} \rightarrow 0$ in ArcFace and, similarly, $\cos \theta_k^p \rightarrow 1$ and $\cos \theta_l^n \rightarrow 0$ in SN-Pair loss. The cosine values in the logit of Equations 2 and 4 are replaced with the ideal values as the probability of a target class in ArcFace and the SN-pair becomes 1.

$$1 \approx \frac{e^{s_1 \cdot \cos m}}{e^{s_1 \cdot \cos m} + C - 1} = 1 - \epsilon \quad (6)$$

$$1 \approx \frac{e^{s_2}}{e^{s_2} + L} = 1 - \epsilon$$

where ϵ is a hyperparameter with a small value to avoid an infinite problem.

By rearranging the equations above, the scale factors s_1 and s_2 are derived with ϵ :

$$s_1 = \frac{\log(1 - \epsilon) + \log(C - 1) - \log \epsilon}{\cos m}, \quad s_2 = \log(1 - \epsilon) + \log L - \log \epsilon \quad (7)$$

Here we define ϵ as a unified scale factor.

5 Experiments

5.1 Implementation Details

Preprocessing. MS1M-RetinaFace (MS1M-R) [6] and K-FACE [27] datasets were used. MS1M-R is a refinement of MS1M [30] with 5.1M images and 93K identities. The K-FACE dataset that we used is summarized in Table 2. Face regions and landmarks were extracted from all the images in MS1M-R and K-FACE using RetinaFace [6]. Then, face alignment was performed based on similarity transformation. All the images were resized to 112×112 and normalized using means [0.485, 0.456, 0.406] and standard deviations [0.229, 0.224, 0.225]. In K-FACE, there are errors in face detection owing to high darkness and low illumination. Fortunately, the face images have similar bounding boxes because they were taken in a strictly controlled environment. Therefore, the bounding boxes and landmarks of erroneous face images were replaced with those of the bright images in L1.

Training. ResNet-34 [1] was chosen as the backbone model. The mini-batch size was set to 512. For the metric loss, 256 positive pairs were randomly sampled from MS1M-R to avoid domination of negative pairs due to a large number of classes, whereas 512 images were randomly sampled from K-FACE because of the small number of classes. The SGD optimizer was employed with a momentum of 0.9 and a weight decay of 0.0005. A cosine annealing scheduler was utilized with a maximum epoch of 20, a warm-up epoch of 3, and an initial learning rate of 0.1.

Testing. The evaluation aimed at face verification, by checking whether two face images belonged to the same class or not. For a face image, a deep feature vector concatenating those of the original and horizontal flip images was used. Two face images were considered to belong to the same class if the cosine similarity between the two images was above a threshold. Performance was measured based on verification accuracy recorded after finding the best threshold in a test dataset automatically.

5.2 Evaluation Results

Model comparison on K-FACE. Table 3 shows the comparison of MixFace and other loss functions on K-FACE. The models were evaluated using $Q_1 - Q_4$ after training with T_4 and selecting the best-performing models on Q_4 as a baseline. FixCos[22] and AdaCos[22] are a hyper-parameter free classification loss. The hyper-parameters for ArcFace were set to $s_1 = 16, m = 0.25$ according to our heuristics. The scale factors in Norm-softmax, CosFace, and SN-pair loss were set to 16. The margin in CosFace was set to 0.25. In the multi-similarity loss [15], MS-loss, the hyper-parameters α, γ , and β were set to 2, 0.5, and 50, respectively. MixFace achieved the best performance on all test datasets, ranging from low to high variances of conditions.

Table 3: Model comparison on K-FACE

Loss function	Q_1	Q_2	Q_3	Q_4
FixCos	98.11	90.47	84.88	80.81
ArcFace	98.30	94.77	87.87	85.41
CosFace	98.20	94.00	89.76	86.57
AdaCos	99.70	95.97	91.17	87.69
N-pair loss	92.40	90.06	88.95	87.15
SN-pair loss	96.90	92.69	89.58	87.70
Ms-loss	99.10	96.30	91.43	88.82
SN-pair loss, ($s_2 = 64$)	99.20	95.01	91.84	89.74
MixFace	100	96.37	92.36	89.80

Unified scale factor. Table 4 shows the effectiveness of the proposed unified scale factor. For a fair experiment, we set the unified scale factor ϵ to 1×10^{-2} and 1×10^{-22} , similar to the value of scale factor s_2 of MixFace. Their settings are approximately (10.84, 16.37) and (58.83, 62.43), respectively. The FR model was not properly trained when s_1 and s_2 were set to (64, 64). The proposed unified scale factor improved the performance in all test datasets compared to using the scale factors s_1 and s_2 independently. These experimental results demonstrate the validity and superiority of the proposed method for adjusting the scale factor ratio for each loss function.

Table 4: Effects of unified scale factor

Loss function	Q_1	Q_2	Q_3	Q_4
MixFace $s_1, s_2 = (16, 16)$	96.80	93.33	89.80	87.33
MixFace $\epsilon = 1 \times 10^{-2}$	98.40	94.06	90.19	88.12
MixFace $s_1, s_2 = (16, 64)$	98.50	94.06	90.55	89.45
MixFace $s_1, s_2 = (64, 64)$	The model is not properly trained			
MixFace $\epsilon = 1 \times 10^{-22}$	100	96.37	92.36	89.80

Comparison with benchmark datasets. Table 5 shows the performance of the three loss functions using various training and test datasets with the same training protocol. Test datasets were evaluated with the best-performing models on LFW. The first three lines were obtained from models trained using MS1M-R. We can see the performance of ArcFace > MixFace > SN-pair loss for all the test datasets. It shows undertraining because the performance of the three models significantly degraded as the variance of conditions increased owing to the rare existence of extreme conditions in MS1M-R.

Interestingly, except for CFP-FP, MixFace > SN-pair > ArcFace according to the second three lines trained with MS1M-R+T4, including fine-grained conditions. This shows that MixFace has strength in fine-grained conditions while also being competitive on benchmark datasets in unconstrained environments. Figure 4 shows the superiority of MixFace using the ROC curves as the ratios between true-positive and false-positive rates are higher than others overall. Figure 5 describes verification accuracies of epochs. Notably, MixFace and SN-pair show similar behaviors on Q4 and LFW, whereas ArcFace produced a competitive performance on LFW but was poor on Q4. It shows the lack of representation power of ArcFace on high variance conditions.

Table 5: Comparison of three loss functions on different test datasets

Loss functions	Train Datasets	Q ₂	Q ₃	Q ₄	LFW	CFP-FP	AgeDB
ArcFace	MS1M-R	98.71	86.60	82.03	99.80	98.41	98.08
SN-pair loss	MS1M-R	92.85	76.36	70.08	99.55	96.20	95.46
MixFace	MS1M-R	97.36	82.89	76.95	99.68	97.74	97.25
ArcFace	MS1M-R+T ₄	76.58	73.13	71.38	99.46	96.75	93.83
SN-pair loss	MS1M-R+T ₄	98.37	94.98	93.33	99.45	94.90	93.45
MixFace	MS1M-R+T ₄	99.27	96.85	94.79	99.53	96.32	95.56

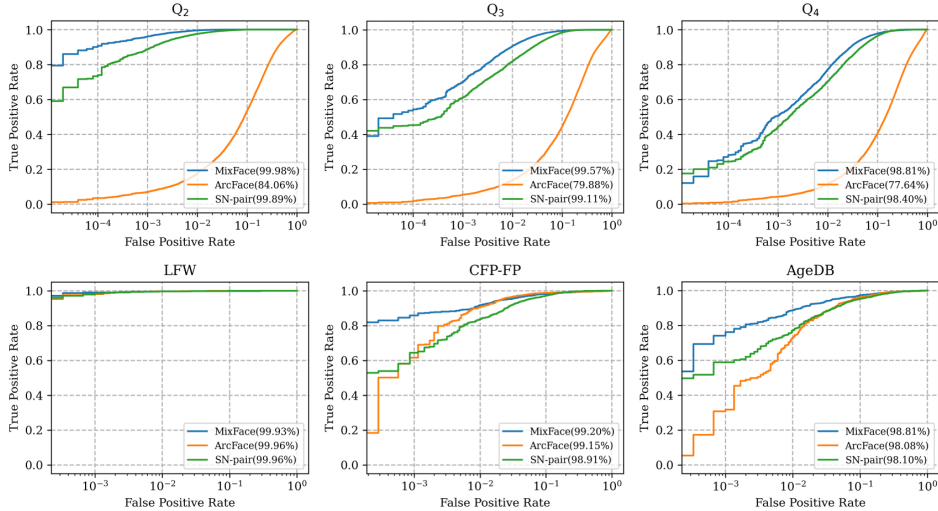


Figure 4: Comparison of ROC curves of models trained with MS1M-R+T₄

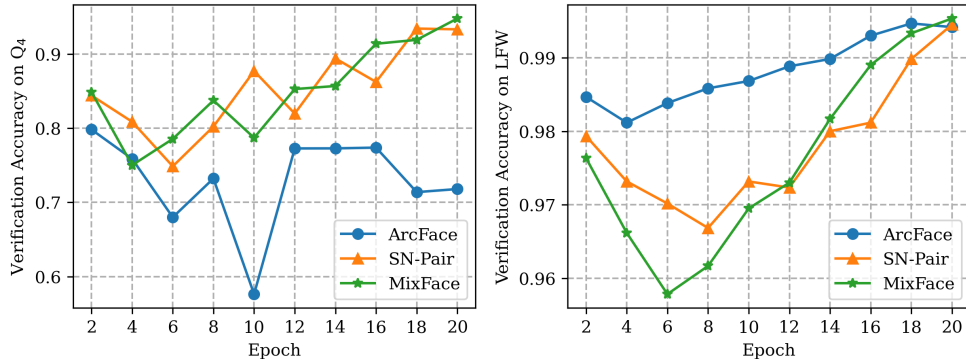


Figure 5: Verification accuracies of epochs on models trained with MS1M-R+T₄

5.3 Effects of Unseen Conditions

Figure 6 shows the heatmaps³ using MixFace with respect to variation of different conditions. Consider a diagonal line P_D and a non-diagonal line P_N of a heatmap. In P_D of the three heatmaps, the differences between the highest and lowest accuracies were small and in the order of accessories (+0.6%) \approx illumination (+0.8%) \approx expression (0.9%). This means that the effect of different conditions of a type on the FR is small. However, the differences between the average accuracies of P_D and P_N are relatively large in the order of illumination (+13.1%) $>$ accessories (+5.6%) $>$ expression (+1.3%). This implies that including unseen conditions in both training and testing considerably affects FR.

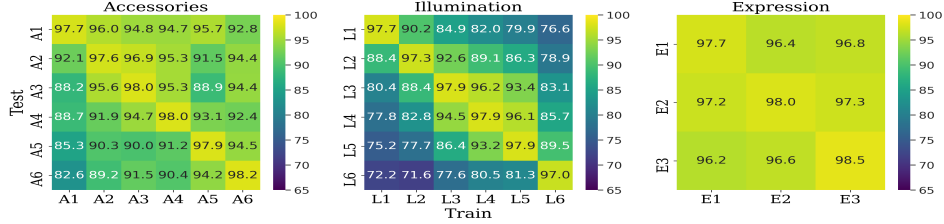


Figure 6: Heatmaps of changing single conditions from (A1,L1,E1,C1-20) (see Table 1). The x- and y-axes denote conversion of a specific condition from the original in training and test datasets, respectively. For the test datasets, we randomly generated 10,000 unique pairs, then converted the corresponding conditions to the y-axis symbols.

6 Conclusion

This paper proposes MixFace, which inherits the benefits of classification and metric losses by analyzing their performance with respect to the variances of conditions in the K-FACE dataset. The superiority of MixFace was demonstrated by a series of experiments on K-FACE and other benchmark datasets, showing that it has strength on various degrees of variance of conditions while maintaining competitiveness on benchmark datasets. In MixFace, manual tuning of hyperparameters can be avoided by presenting a unified scale factor. We expect MixFace to be a good option for surveillance tasks with fine-grained conditions. In our future work, we plan to investigate various methods of mixing classification and metric losses.

7 Acknowledgement

This work was supported by the National Research Foundation of Korea (NRF) grant funded by the Korea government (MSIT) (No. NRF-2019R1G1A1003312) and (No. NRF-2021R1I1A3052815).

References

- [1] Kaiming He, Xiangyu Zhang, Shaoqing Ren, and Jian Sun. Deep residual learning for image recognition. In *2016 IEEE Conference on Computer Vision and Pattern Recognition, CVPR 2016, Las Vegas, NV, USA, June 27-30, 2016*, pages 770–778, 2016.
- [2] Jie Hu, Li Shen, Samuel Albanie, Gang Sun, and Enhua Wu. Squeeze-and-excitation networks. *IEEE Trans. Pattern Anal. Mach. Intell.*, 42(8):2011–2023, 2020.
- [3] Karen Simonyan and Andrew Zisserman. Very deep convolutional networks for large-scale image recognition. *arXiv preprint arXiv:1409.1556*, 2014.
- [4] Christian Szegedy, Wei Liu, Yangqing Jia, Pierre Sermanet, Scott E. Reed, Dragomir Anguelov, Dumitru Erhan, Vincent Vanhoucke, and Andrew Rabinovich. Going deeper with convolutions. In *IEEE Conference on Computer Vision and Pattern Recognition, CVPR 2015, Boston, MA, USA, June 7-12, 2015*, pages 1–9, 2015.

³Similar results were observed using ArcFace and SN-pair, respectively.

- [5] Fei Wang, Liren Chen, Cheng Li, Shiyao Huang, Yanjie Chen, Chen Qian, and Chen Change Loy. The devil of face recognition is in the noise. In *Proceedings of the European Conference on Computer Vision (ECCV)*, pages 765–780, 2018.
- [6] Jiankang Deng, Jia Guo, Evangelos Ververas, Irene Kotsia, and Stefanos Zafeiriou. Retinaface: Single-shot multi-level face localisation in the wild. In *Proceedings of the IEEE/CVF Conference on Computer Vision and Pattern Recognition*, pages 5203–5212, 2020.
- [7] Qiong Cao, Li Shen, Weidi Xie, Omkar M Parkhi, and Andrew Zisserman. Vggface2: A dataset for recognising faces across pose and age. In *2018 13th IEEE international conference on automatic face & gesture recognition (FG 2018)*, pages 67–74. IEEE, 2018.
- [8] Sumit Chopra, Raia Hadsell, and Yann LeCun. Learning a similarity metric discriminatively, with application to face verification. In *2005 IEEE Computer Society Conference on Computer Vision and Pattern Recognition (CVPR’05)*, volume 1, pages 539–546. IEEE, 2005.
- [9] Raia Hadsell, Sumit Chopra, and Yann LeCun. Dimensionality reduction by learning an invariant mapping. In *2006 IEEE Computer Society Conference on Computer Vision and Pattern Recognition (CVPR’06)*, volume 2, pages 1735–1742. IEEE, 2006.
- [10] Omkar M. Parkhi, Andrea Vedaldi, and Andrew Zisserman. Deep face recognition. In *Proceedings of the British Machine Vision Conference 2015, BMVC 2015, Swansea, UK, September 7-10, 2015*, pages 41.1–41.12, 2015.
- [11] Florian Schroff, Dmitry Kalenichenko, and James Philbin. Facenet: A unified embedding for face recognition and clustering. In *Proceedings of the IEEE conference on computer vision and pattern recognition*, pages 815–823, 2015.
- [12] Yaniv Taigman, Ming Yang, Marc’Aurelio Ranzato, and Lior Wolf. Deepface: Closing the gap to human-level performance in face verification. In *Proceedings of the IEEE conference on computer vision and pattern recognition*, pages 1701–1708, 2014.
- [13] Yandong Wen, Kaipeng Zhang, Zhifeng Li, and Yu Qiao. A discriminative feature learning approach for deep face recognition. In *European conference on computer vision*, pages 499–515. Springer, 2016.
- [14] Kihyuk Sohn. Improved deep metric learning with multi-class n-pair loss objective. In *Proceedings of the 30th International Conference on Neural Information Processing Systems*, pages 1857–1865, 2016.
- [15] Xun Wang, Xintong Han, Weilin Huang, Dengke Dong, and Matthew R Scott. Multi-similarity loss with general pair weighting for deep metric learning. In *Proceedings of the IEEE/CVF Conference on Computer Vision and Pattern Recognition*, pages 5022–5030, 2019.
- [16] Jiankang Deng, Jia Guo, Niannan Xue, and Stefanos Zafeiriou. Arcface: Additive angular margin loss for deep face recognition. In *Proceedings of the IEEE/CVF Conference on Computer Vision and Pattern Recognition*, pages 4690–4699, 2019.
- [17] Hao Wang, Yitong Wang, Zheng Zhou, Xing Ji, Dihong Gong, Jingchao Zhou, Zhifeng Li, and Wei Liu. Cosface: Large margin cosine loss for deep face recognition. In *Proceedings of the IEEE conference on computer vision and pattern recognition*, pages 5265–5274, 2018.
- [18] Weiyang Liu, Yandong Wen, Zhiding Yu, Ming Li, Bhiksha Raj, and Le Song. Spherenet: Deep hypersphere embedding for face recognition. In *Proceedings of the IEEE conference on computer vision and pattern recognition*, pages 212–220, 2017.
- [19] Feng Wang, Jian Cheng, Weiyang Liu, and Haijun Liu. Additive margin softmax for face verification. *IEEE Signal Processing Letters*, 25(7):926–930, 2018.
- [20] Ben Harwood, Vijay Kumar BG, Gustavo Carneiro, Ian Reid, and Tom Drummond. Smart mining for deep metric learning. In *Proceedings of the IEEE International Conference on Computer Vision*, pages 2821–2829, 2017.
- [21] Weifeng Ge. Deep metric learning with hierarchical triplet loss. In *Proceedings of the European Conference on Computer Vision (ECCV)*, pages 269–285, 2018.
- [22] Xiao Zhang, Rui Zhao, Yu Qiao, Xiaogang Wang, and Hongsheng Li. Adacos: Adaptively scaling cosine logits for effectively learning deep face representations. In *Proceedings of the IEEE/CVF Conference on Computer Vision and Pattern Recognition*, pages 10823–10832, 2019.

- [23] Baosheng Yu and Dacheng Tao. Deep metric learning with triplet margin loss. In *Proceedings of the IEEE/CVF International Conference on Computer Vision*, pages 6490–6499, 2019.
- [24] Gary B Huang, Marwan Mattar, Tamara Berg, and Eric Learned-Miller. Labeled faces in the wild: A database for studying face recognition in unconstrained environments. In *Workshop on faces in 'Real-Life' Images: detection, alignment, and recognition*, 2008.
- [25] Soumyadip Sengupta, Jun-Cheng Chen, Carlos Castillo, Vishal M Patel, Rama Chellappa, and David W Jacobs. Frontal to profile face verification in the wild. In *2016 IEEE Winter Conference on Applications of Computer Vision (WACV)*, pages 1–9. IEEE, 2016.
- [26] Stylianos Moschoglou, Athanasios Papaioannou, Christos Sagonas, Jiankang Deng, Irene Kotsia, and Stefanos Zafeiriou. Agedb: the first manually collected, in-the-wild age database. In *Proceedings of the IEEE Conference on Computer Vision and Pattern Recognition Workshops*, pages 51–59, 2017.
- [27] Yeji Choi, Hyunjung Park, Gi Pyo Nam, Haksub Kim, Heeseung Choi, Junghyun Cho, and Ig-Jae Kim. K-face: A large-scale kist face database in consideration with unconstrained environments. *arXiv preprint arXiv:2103.02211*, 2021.
- [28] Yifan Sun, Changmao Cheng, Yuhang Zhang, Chi Zhang, Liang Zheng, Zhongdao Wang, and Yichen Wei. Circle loss: A unified perspective of pair similarity optimization. In *Proceedings of the IEEE/CVF Conference on Computer Vision and Pattern Recognition*, pages 6398–6407, 2020.
- [29] James Bergstra and Yoshua Bengio. Random search for hyper-parameter optimization. *Journal of machine learning research*, 13(2), 2012.
- [30] Yandong Guo, Lei Zhang, Yuxiao Hu, Xiaodong He, and Jianfeng Gao. Ms-celeb-1m: A dataset and benchmark for large-scale face recognition. In *European conference on computer vision*, pages 87–102. Springer, 2016.